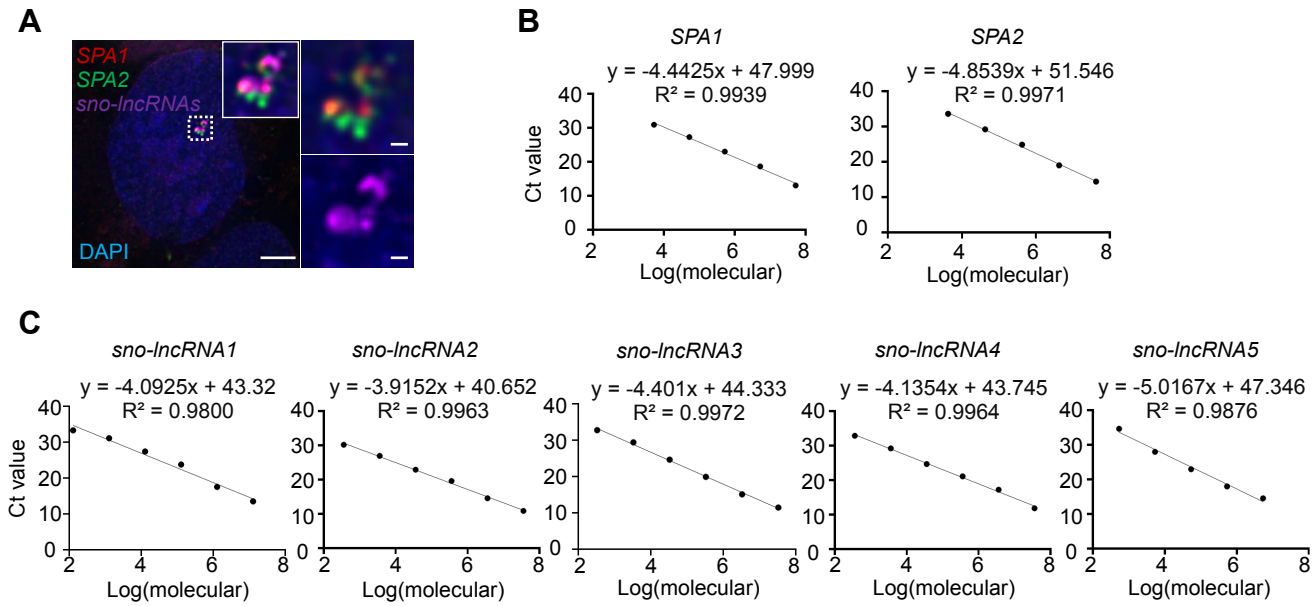

Figure S1. The localization and copy number evaluation of *SPA*s and *sno-lncRNA*s.

(A) Representative RNA FISH images of *SPA*s and *sno-lncRNA*s in H9 cells. Scale bar, 5 μm (uncropped) and 500 nm (cropped).

(B) The standard curves for *SPA1* and *SPA2* generated from *in vitro* purified RNA fragments.

(C) The standard curves for *sno-lncRNA*s generated from *in vitro* purified RNA fragments.

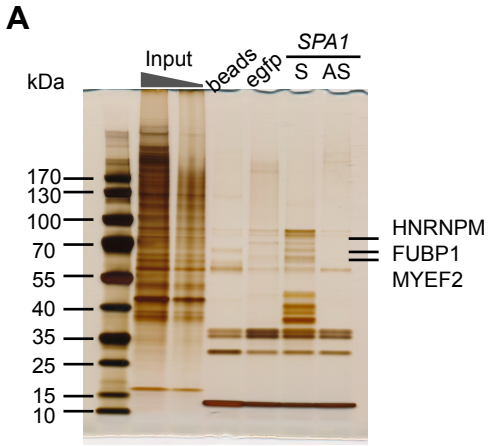

B

Protein names	Peptides_ *SPA1*-AS	Peptides_ *SPA1*-S	ΔPeptides S-AS
FUBP3	0	26	26
RBMX	0	26	26
HNRNPR	0	21	21
RBMXL1	0	18	18
KHSRP	0	17	17
IGF2BP1	0	16	16
FUBP1	0	16	16
ADAR	0	14	14
HNRNPA1	3	17	14
IGF2BP2	0	13	13
HNRNPA2 B1	4	14	10
IGF2BP3	0	9	9
ELAVL1	0	9	9
HNRNPL	4	13	9
MYEF2	0	8	8
HNRNPM	11	19	8
HNRNPD	1	9	8
PTBP1	0	7	7
HNRNPC	3	10	7
PUM2	0	4	4

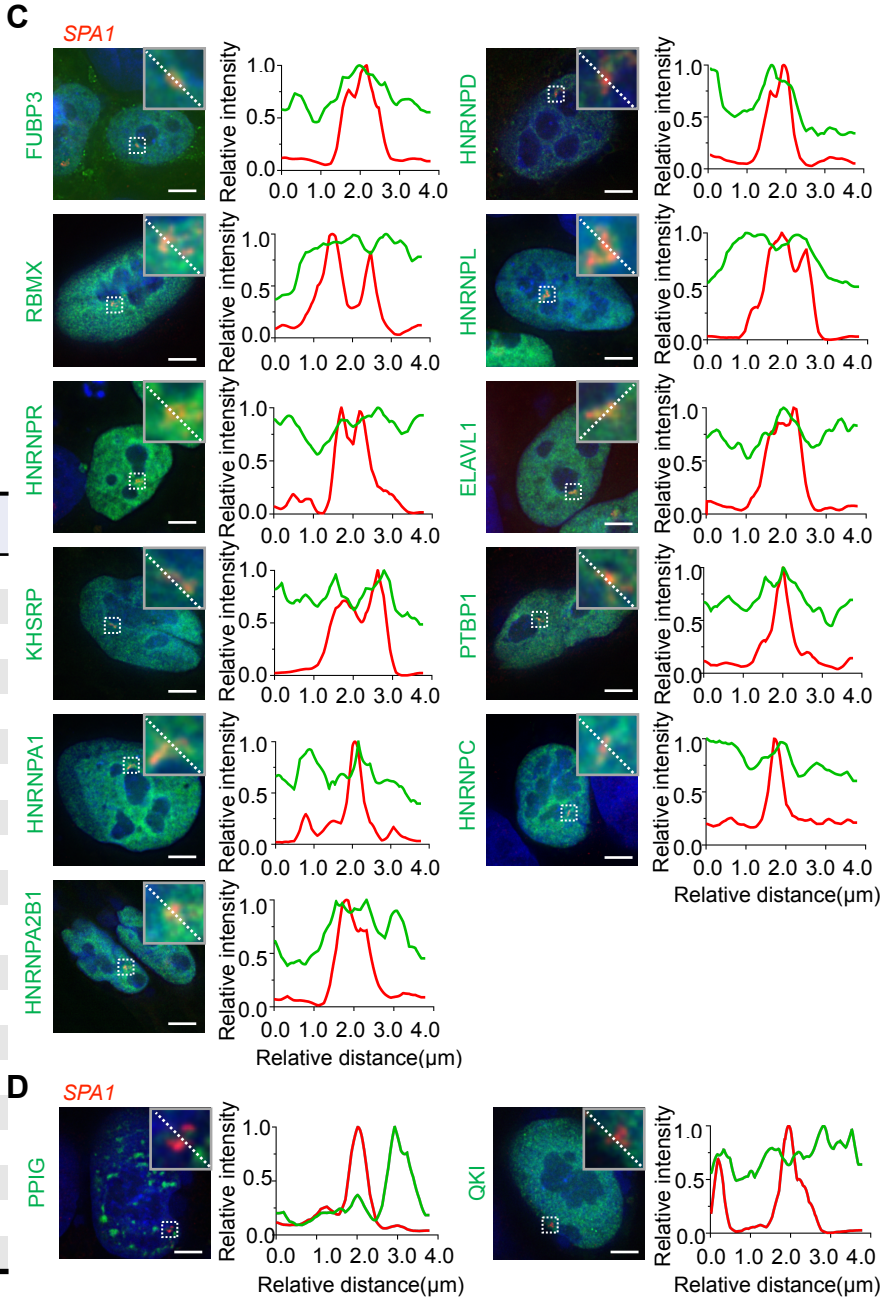

Figure S2. The localization patterns of the *SPA1*-interacting proteins.

(A) The silver staining showing the *SPA1* pull-down quality. The potential bands of FUBP1, MYEF2, and HNRNPM are indicated.

(B) The top 20 proteins identified from the *SPA1* pull-down followed by MS. Duplicated biological experiments are performed. The average peptides pulled down by *SPA1*-AS and *SPA1*-S probes are shown in the table. HNRNPM (highlighted in blue) is a reported splicing factor that accumulates in the PWS bodies. FUBP1 and MYEF2 (highlighted in red) are newly identified proteins that also accumulate there.

(C) *SPA1* does not co-localize with the *SPA1*-interacting proteins revealed from (B), except FUBP1, MYEF2, and HNRNPM, revealed by *SPA1* and corresponding protein staining. Scale bar, 5 μm.

(D) *SPA1* does not co-localize with PPIG or QKI, revealed by *SPA1* and corresponding protein staining. Scale bar, 5 μm.

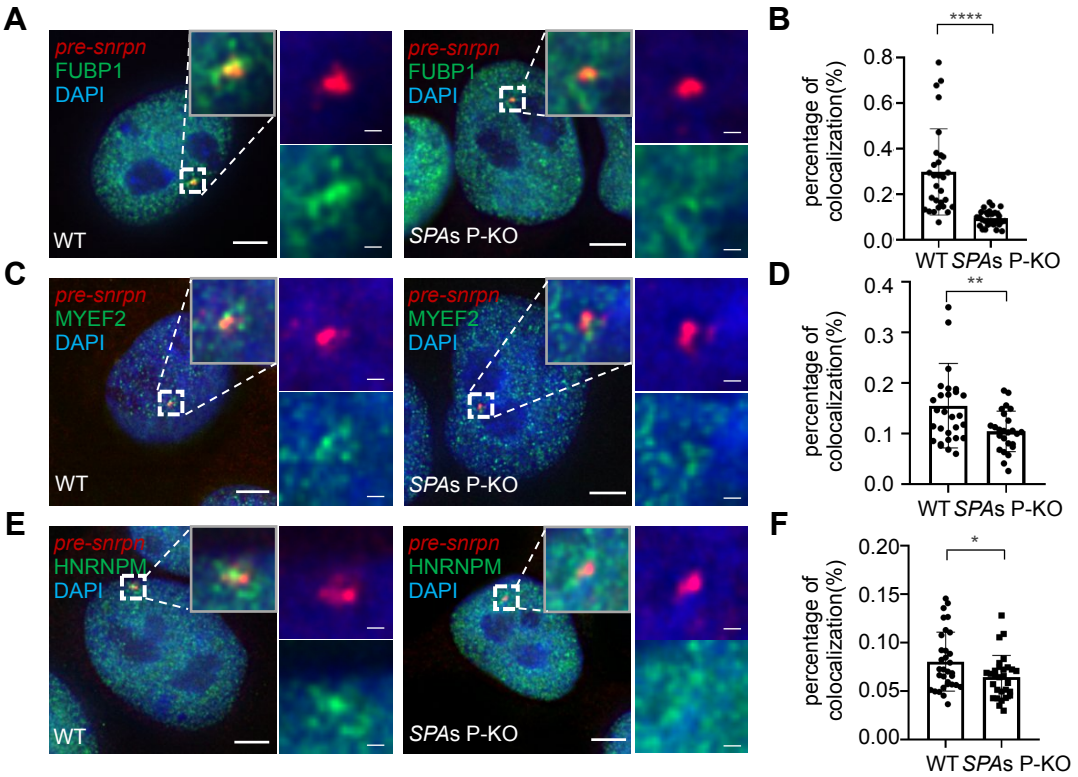

Figure S3. *SPA*s enrich FUBP1, MYEF2 and HNRNPM in the PWS bodies in PA1 cells.

(A) The representative images showing the localization of FUBP1 and *pre-snrpn* in WT and *SPA*s P-KO PA1 cells. Scale bar, 5 μm (uncropped) and 500 nm (cropped). *pre-snrpn* is stained as the marker of PWS bodies.

(B) Percentage of FUBP1 co-localized with *pre-snrpn* in WT and *SPA*s P-KO PA1 cells. n=29 WT and n=30 *SPAs* P-KO cells are used for evaluation.

(C) The representative images showing the localization of MYEF2 and *pre-snrpn* in WT and *SPA*s P-KO PA1 cells. Scale bar, 5 μm (uncropped) and 500 nm (cropped). *pre-snrpn* is stained as the marker of PWS bodies.

(D) Percentage of MYEF2 co-localized with *pre-snrpn* in WT and *SPA*s P-KO PA1 cells. n=29 WT and n=25 *SPAs* P-KO cells are used for evaluation

(E) The representative images showing the localization of HNRNPM and *pre-snrpn* in WT and *SPA*s P-KO PA1 cells. Scale bar, 5 μm (uncropped) and 500 nm (cropped). *pre-snrpn* is stained as the marker of PWS bodies.

(F) Percentage of HNRNPM co-localized with *pre-snrpn* in WT and *SPA*s P-KO PA1 cells. n=33 WT and n=29 *SPAs* P-KO cells are used for evaluation.

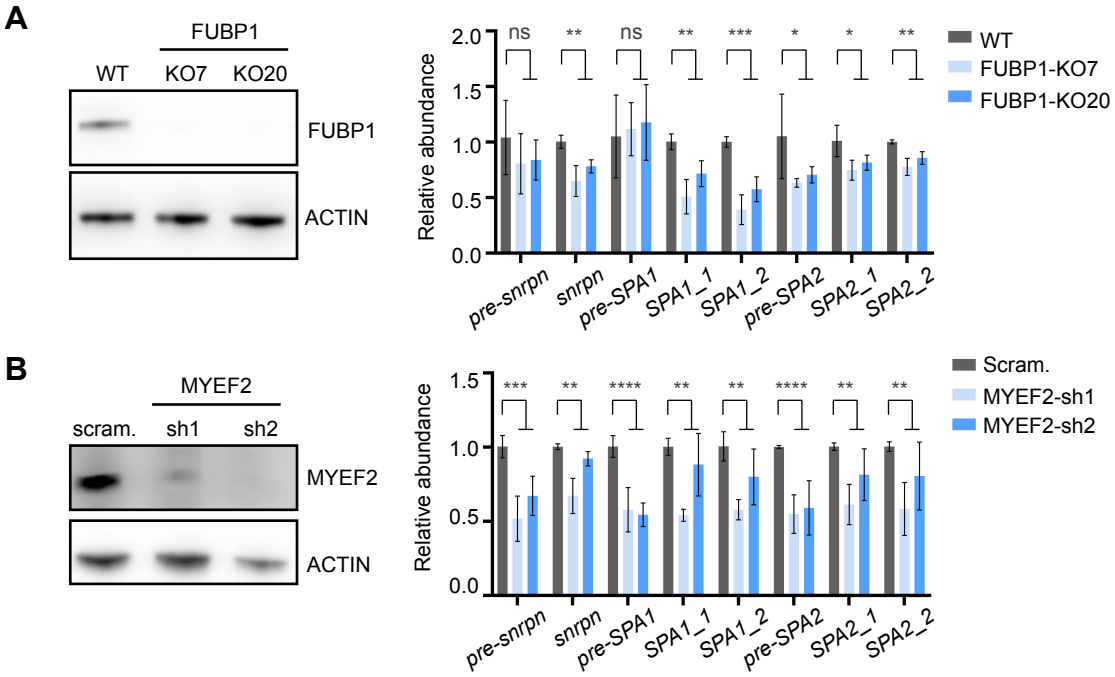

Figure S4. FUBP1 or MYEF2 depletion mildly impairs expression of *SPA*s in H9 cells.

(A) Knockdown of FUBP1 mildly affects the expression of *SPA*s in H9 cells. Left, knockdown efficiency of FUBP1 analyzed by western blotting. Right, the expression levels of *pre-snrpn*, *snrpn*, *pre-SPA*s, and *SPA*s detected by RT-qPCR.

(B) Knockdown of MYEF2 mildly affects the expression of *SPA*s in H9 cells. Left, knockdown efficiency of MYEF2 analyzed by western blotting. Right, the expression levels of *pre-snrpn*, *snrpn*, *pre-SPA*s, and *SPA*s detected by RT-qPCR.

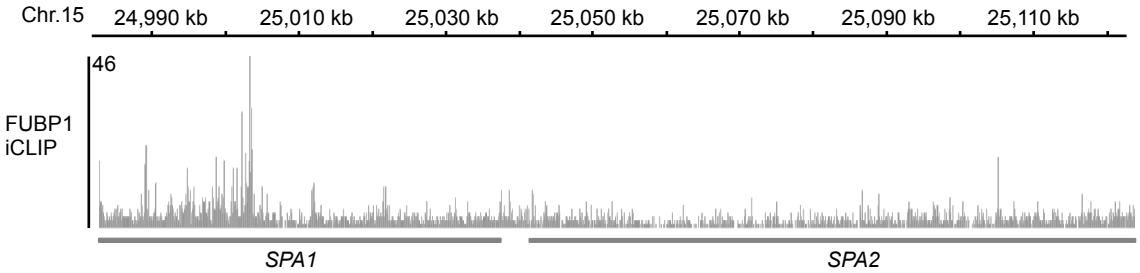

Figure S5. FUBP1 binds to the *SPA1* but not *SPA2*.

FUBP1 iCLIP-seq results (GEO: GSE220184) (Ebersberger et al. 2023) showing that FUBP1 has strong binding to the *SPA1* but not *SPA2*.